

Dose and time-dependent tolerability and efficacy of organo-osmium complex FY26 and its tissue pharmacokinetics in hepatocarcinoma-bearing mice

Authors:

Swati A Kumar^{1,2}, Russell J. Needham³, Kristin Abraham¹, Hannah E Bridgewater³, Lauren A Garbutt¹, Helena Xandri-Monje¹, Robert Dallmann¹, Sebastien Perrier³, Peter J. Sadler³ and Francis Lévi^{1,4,5}

¹ Chronotherapy Team, Division of Biomedical Sciences, Warwick Medical School, University of Warwick, Gibbett Hill Road, Coventry, CV4 7AL, United Kingdom

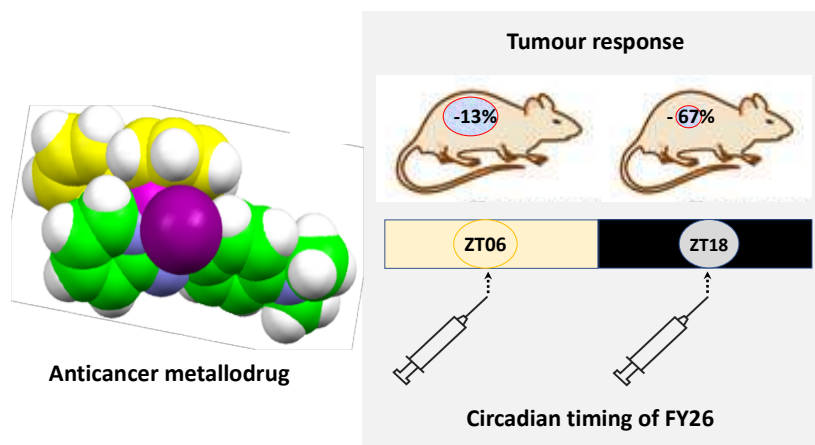
² Present address: Cell and Developmental Biology, University College London, London, WC1E 6BT, United Kingdom.

³ Department of Chemistry, University of Warwick, Coventry, CV4 7AL, United Kingdom.

⁴ UPR “ Chronotherapy, Cancers and Transplantation”, Faculty of Medicine, Paris Saclay University, Campus CNRS, 7 rue Guy Moquet, 94800 - Villejuif, France.

⁵ Hepato-Biliary Center, Paul Brousse Hospital, Assistance Publique-Hopitaux de Paris (AP-HP), 12-14 Avenue Paul-Vaillant Couturier, 94800 - Villejuif, France

TABLE OF CONTENTS



In vivo efficacy and tolerability of this inert organo-osmium anticancer complex is dependent on the time of administration (day versus night), consistent with preferential activation at specific stages of the circadian cycle.

ABSTRACT

The organo-osmium complex $[\text{Os}^{\text{II}}(\eta^6\text{-}p\text{-cym})(\text{PhAzPy-NMe}_2)\text{I}]^+$ (FY26) exhibits promising *in vitro* antitumour activity against mouse hepatocarcinoma Hepa1-6 and other mouse or human cancer cell lines. Here, we drastically enhance water solubility of FY26 through the replacement of the PF_6^- counter-anion with chloride using a novel synthesis method. FY26. PF_6 and FY26.Cl displayed similar *in vitro* cytotoxicity in two cancer cell models. We then show the moderate and late anticancer efficacy of FY26. PF_6 and FY26.Cl in a subcutaneous murine hepatocarcinoma mouse model. Both efficacy and tolerability varied according to FY26 circadian dosing time in hepatocarcinoma tumour-bearing mice. Tumour and liver uptake of the drug were determined over 48 h following FY26.Cl administration at Zeitgeber 6 (ZT6), when the drug is least toxic (in the middle of the light span when mice are resting). Our studies suggest the need to administer protracted low doses of FY26 at ZT6 in

order to optimize its delivery schedule, for example through the use of chrono-releasing nanoparticles.

SIGNIFICANCE TO METALLOMICS STATEMENT

Metallodrugs differ from most organic drugs in that they are prodrugs, which undergo transformation by ligand substitution and redox reactions before reaching target sites. Here we study the *in vitro* and *in vivo* efficacy of an organo-osmium anticancer complex FY26 – a relatively inert complex activated in cancer cells by attack on its azo-bond by the tripeptide glutathione. We find that the efficacy and tolerability of FY26.PF₆ or FY26.Cl are dependent on the time of administration, consistent with a role for the circadian clock in controlling expression of genes involved in glutathione synthesis .

INTRODUCTION

There is a need for anticancer drugs with new mechanisms of action to complement platinum drugs in the clinic, reduce side-effects and overcome emerging platinum resistance. Complexes of ruthenium have been investigated in clinical trials,^{1, 2} and compounds of heavier congener osmium are being explored.^{3, 4} Although in the same periodic group, and often possessing complexes of similar composition (oxidation state, ligand set, size and geometry), the reactivity of ruthenium and osmium complexes can differ markedly. Notably, organo-Os(II) arene complexes hydrolyse much more slowly and bound water ligands are more acidic.⁵

Numerous experimental and clinical studies have highlighted the relevance of circadian timing in drug administration for the optimisation of pharmacological effects.^{6, 7} For instance, dosing an anticancer medication at a specific time with reference to circadian rhythms can increase or decrease both efficacy and tolerability.⁸⁻¹⁰ As demonstrated for 28 anticancer agents belonging to various classes, the administration of a drug at the circadian time when it is best tolerated often achieves best antitumour activity.^{6, 7, 9, 10} Here we sought the relevance of this chronopharmacological principle along preclinical developmental stages of organo-Os complexes.

Organometallic half-sandwich Os(II) arene complexes with phenylazopyridine (PhAzPy) bidentate ligands show promising anticancer activity *in vitro* against a variety of cancer cell lines,^{11, 12} and also *in vivo*.¹³ In contrast to less-active organo-Os(II) drugs with *N,N*-chelated diamine or *N,O*-chelated picolinate ligands, which rely primarily on the dissociation of labile ligands followed by DNA binding.^{14, 15} Iodido Os(II) PhAzPy complexes are considerably more stable in aqueous media and exhibit a mechanism of activity involving intracellular ROS production. These inert complexes are activated in cancer cells by attack of glutathione on the azo bond of the chelated PhAzPy ligand.^{16, 17} A key complex, FY26.PF₆ ([Os^{II}(η^6 -*p*-cym)(PhAzPy-NMe₂)I]PF₆), is on average 49 times more active than cisplatin in the 809 cancer cell line screen of the Sanger Institute,¹⁸ and capable of delaying the

growth of HCT-116 human colon cancer xenografts in mice.¹³ Furthermore, it is up to 64 times more selective towards A2780 ovarian cancer cells over MRC5 fibroblasts when applied synergistically with L-buthionine-sulfoximine.¹⁹ The structure of FY26 and its biomolecular mechanism of action are shown in Figure 1.

In vitro experiments have also demonstrated time-dependent efficacy of FY26.PF₆ against both mouse Hepa1-6 hepatocarcinoma and human HCT116 colon carcinoma in cell cultures in **Figure 1A**.²⁰ More specifically, the IC₅₀ of FY26.PF₆ varied by 40% according to the timing of *in vitro* drug exposure of cultured Hepa1-6 cells, following the synchronization of their circadian clocks with a 24-h periodic temperature cycle.^{20, 21} The least toxic timing for FY26.PF₆ administration was near the minimum of the sinusoidal temperature cycle which synchronizes the genetic circadian clocks of the cells in the Petri dishes over the 24 hours. FY26.PF₆ chronopharmacology mechanisms depend upon clock gene Bmal1 proficiency, and involve circadian dependent FY26 uptake and possibly efflux². Moreover, the toxicity of FY26.PF₆ also varies according to dosing time in mice.²¹ The best tolerated time for FY26 in mice following dosing is near the middle of the light span, which corresponds to the low point in their endogenous circadian rhythm in core body temperature. Strikingly, the circadian rhythm in FY26.PF₆ toxicity for Hepa1-6 cells and for mice differs from those in oxaliplatin toxicity by several hours, hence further highlighting the pharmacological differences between these organo-osmium complexes and platinum metallodrugs on the temporal timescale.²¹

Here we aimed to optimize the chemical solubility of FY26 prior to the determination of FY26 efficacy and tolerability in Hepa1-6 tumour-bearing mice. We further obtained insight in to its tissue uptake, so as to optimize its dosing schedule, both in terms of the frequency of administration and circadian timing.

METHODS

FY26 synthesis and characterisation

FY26.PF₆ was synthesised and characterised as previously reported,¹² however, it was poorly water soluble. We previously reported that the anion (X) has a major effect on aqueous solubility for organo-osmium complexes.²² Here we synthesised FY26 as a chloride salt (FY26.Cl) instead of PF₆. Furthermore, the route by which FY26 is synthesised was improved upon, now involving a 2-step one pot synthesis from [Os(η^6 -*p*-cym)Cl₂]₂. FY26 was firstly isolated as an iodide salt (FY26.I), which is an important purification step prior to anion exchange with chloride. The anion exchange was conducted by passing FY26.I through Dowex® 1X4 chloride form resin, yielding FY26.Cl.

Synthesis of FY26.Cl

[Os(η^6 -*p*-cym)Cl₂]₂ (4.0 g, 5.06 mmol) was dissolved in methanol (50 mL) and heated to 80 °C. A solution of potassium iodide (84.0 g, 505.91 mmol) in water (50 mL) was added and the mixture stirred for 5 min. A solution of *N,N*-dimethyl-4-(2-pyridylazo)aniline (2.4 g, 10.62 mmol) in methanol (50 mL) was added drop-wise and the mixture was stirred for 1 h at 80 °C, and left stirring for 18 h at ambient temperature. The majority of methanol was removed under reduced pressure using a rotavap and the product was extracted with dichloromethane (100 mL), and washed with water (100 mL). More product was extracted from the aqueous layer with dichloromethane washings (4 × 50 mL). The combined dichloromethane extracts were vacuum filtered to remove a black impurity, and the filtrate was dried under reduced pressure. The solids were fully redissolved in a mixture of ethanol (200 mL) and dichloromethane (50 mL). The volume of the solution was reduced using a rotavap to ~40 mL and a precipitate formed, then the mixture was placed in a freezer (-20 °C) overnight. The intermediate product (FY26.I) was collected via vacuum filtration and washed with ice-cold ethanol (~10 mL), then diethyl ether (6 × 50 mL). The washes were repeated once more. FY26 was collected, analysed by HPLC (99.4% pure. C18 column; 250 x 4.6 mm and pore size = 5 µm.

Mobile phase; acetonitrile/water + 0.1% trifluoroacetic acid), and dissolved in methanol (100-150 mL).

A chromatography column (250 mL) containing Dowex® 1X4 chloride form resin was prepared (Sigma-Aldrich, Dorset, UK). The resin was flushed with aqueous sodium chloride solution (0.1 g/mL, 0.8 L), water (1.0 L), methanol:water (1:1, v/v, 0.8 L), then methanol (0.4 L). The FY26.I methanol solution was passed through the column using methanol as an eluent. The dark-blue complex was collected and any other fractions were discarded. The extract was evaporated to dryness under reduced pressure, and the solids were redissolved in a minimum volume of dichloromethane. This was dried once more under reduced pressure, forming a shiny flaky dark-blue amorphous solid, which was isolated and dried overnight in a vacuum desiccator. Yield: (7.09 g, 98%). ¹H NMR ((CD₃)CO): δ 9.91-9.93 (m, 1H), 8.56-8.58 (m, 1H), 8.15-8.22 (m, 3H), 7.56-7.60 (m, 1H), 6.93-6.95 (m, 2H), 6.81-6.82 (m, 1H), 6.68-6.70 (m, 1H), 6.34-6.36 (m, 1H), 6.28-6.29 (m, 1H), 3.35 (s, 6H), 2.77 (s, 3H), 2.52 (sept., 1H, J = 6.9 Hz), 0.97 (d, 3H, J = 6.9 Hz), 0.91 (d, 3H, J = 6.9 Hz). ESI-MS calculated for C₂₃H₂₈IN₄Os⁺: m/z 679.1. Found: 679.1. CHN and Cl analysis: Found: C, 38.99%; H, 4.57%; N, 7.22%; Cl, 4.69%. Calculated for C₂₃H₂₈ClIN₄Os: C, 38.74%; H, 3.96%; N, 7.86%; Cl, 4.97%. HPLC purity: 99.1%.

Comparative solubility study

One to 5 mg of FY26.PF₆ or FY26.I, and 180 mg FY26.Cl was dispensed into falcon tubes in triplicates, then 1 mL of doubly deionised water was added. The falcon tubes were placed on a Vibrax VXB basic shaker (Sigma-Aldrich, Dorset, UK) for 24 h at a speed of 500 g/min (ambient temperature 18-20 °C), and were checked at intervals (further solids were added if total saturation appeared to occur). The samples were filtered through syringe filters (PTFE, 0.45 µm, 4 mm) to remove any undissolved solids. The concentrations of the solutions (Os) were measured using inductively coupled plasma-optical emission spectroscopy (ICP-OES) (Agilent, Stockport, UK).

Separation of FY26 enantiomer via chiral HPLC

A solution of FY26 in EtOH (1 mg/mL) was prepared and filtered through a syringe filter (PTFE, 4 mm x 0.45 µm). Preparative chiral HPLC was carried out using an Agilent Technologies 1200 series HPLC instrument with a VWD and 1 mL loop. The instrument was fitted with a DAICEL Group (Chiral Technologies Europe) Chiralpak IC cellulose-based semi-preparative column (250 x 10 mm, 5 µm pore size), and a guard column (Same brand and stationary phase; 10 x 20 mm, 5 µm pore size). The mobile phase consisted of EtOH:n-heptane (1:1, v/v), with 0.5% trimethylamine (TEA, v/v) and 0.3% trifluoroacetic acid (TFA, v/v) additives. The mobile phase was isocratic with a flow rate of 3 mL/min. Aliquots of 40× of 500 µL were injected manually with a sample run time of 30 min (wavelength of detection = 254 nm). Two distinct peaks were observed at retention times 17.9 min (enantiomer 1) and 20.3 min (enantiomer 2), and collected manually. Combined fractions were evaporated to dryness, re-dissolved in MeCN:H₂O (1:9, v/v, 10 mL), and purified by preparative reverse-phase HPLC to remove excess TEA and its salts. Excess NH₄PF₆ (~100 mol equiv) was combined with each enantiomer and the HPLC solvents were removed under reduced pressure. The enantiomers were dissolved in DCM (5 mL), filtered, dried under vacuum, and stored in a freezer (-20 °C).

Biological Assays

A first *in vitro* study investigated the relevance of iodide or chloride anion for the maximum solubility and cytotoxicity of FY26. Five *in vivo* experiments (Exp 1 to 5) were performed involving a total of 170 mice in order to determine (i) the antitumour efficacy of FY26 against measurable hepatocarcinoma (Hepa1-6-Per2-luc); (ii) the possible limiting toxicity and the influence of dosing time; and (iii) the relationship between dose level and tumour and liver drug uptake (**Table 1**).

Cell culture

Dulbecco's Modified Eagle's Medium (DMEM) cell culture media, penicillin/streptomycin, foetal bovine serum, L-glutamine, phosphate buffered saline solution (PBS) and trypsin/EDTA were all purchased from Thermo Fisher (Loughborough, UK). DMEM was supplemented with 10% foetal bovine serum, 1% penicillin/streptomycin and 2mM L-glutamine. Cancer cell lines (A2780 and A549) were purchased from the European Collection of Cell Cultures (Salisbury, UK). Cell cultures were grown in T-75 or T-175 culture flasks as adherent monolayers. The cells were passaged 2-3 times per week whenever confluence reached 80-90%, using 0.25% trypsin/EDTA. Cell cultures were stored in an incubator at 37 °C with a 5% CO₂ humidified atmosphere.

In vitro growth inhibition assay

Five thousand A2780 or A549 cells were seeded per well in 96-well plates. The cells were pre-incubated in drug-free media at 37 °C for 48 h before adding a range of concentrations (0.01-100 µM) of the complexes to be tested. Typically, the complex was dissolved in DMSO at 2 mM concentration, then diluted with cell culture medium to give a 100 µM stock solution with 5% v/v DMSO. Cells were exposed to complexes for 24 h at 37 °C. The supernatants were removed by suction and each well was washed with PBS. The cells were allowed to recover for 72 h in a drug-free medium at 37 °C. The SRB assay was used to determine cell viability²³. Absorbance measurements of the solubilised dye (Thermo Scientific Multiskan FC with SkanIt software 4.1 for Windows using a 470 nm filter) allowed the determination of viable treated cells compared to untreated controls. IC₅₀ values (the concentration at which 50% cell death occurs) were determined as triplicates of duplicates for each complex. ICP-OES was used to determine the osmium concentrations of the initial stock solutions of the complexes, and the IC₅₀ values were corrected accordingly.

ICP-OES

Analyses of FY26 solutions were carried out on a Perkin Elmer (Optical Emission Spectrometer) Optima 5300 DV instrument. All samples and standards were prepared fresh on the day in doubly deionised water with distilled HNO₃ (3.2%), thiourea (5 mM), and ascorbic acid (0.1 g/L). The osmium standard was diluted to the following concentrations for the calibration curve: 0, 25, 50, 100, 200, 400, 600, 800 and 1000 ppb. The samples were diluted by serial dilutions of typically 1 in 10 until their concentrations fitted within the calibration range and % total dissolved solids were below 0.2%. Samples were prepared in triplicates and the Os optical emissions at 228.226 and 225.585 nm were detected and integrated.

Animals

Male CD1-*Foxn1*^{nu} or C57Bl/6 (B6) mice aged 5-10 weeks (Janvier, Le Genest St Isle, France) were housed in groups of 3-4 mice per cage in temperature-controlled (23 ± 1 °C), ventilated (100 ± 10 L/min) and light tight chronobiologic animal facilities (Eurobioconcept, Bonneuil s/Marne, France). They were synchronized with an alternation of 12 h of light (L) and 12 h of darkness (D) (LD12:12), with light starting at 07:00, and had *ad libitum* access to food and water throughout all the experiments. In line with convention, onset of light and that of darkness are referred to as Zeitgeber Time 0 (ZT0) and ZT12, respectively. After one or more weeks on this regimen and on the day prior to tumour inoculation, both flanks of each B6 mouse were shaved using clippers.

Tumour inoculation and growth assessment

Mouse hepatocarcinoma (Hepa1-6, ATCC® CRL-1830™) were kindly provided by S. Dulong (INSERM U935, Villejuif, France), following their stable transfection with the *Per2-luc* (pLV7-Bsd-P(*Per2*)-dLuc) reporter constructs within the C5SYS ERASYSBIO+ project (FP7). Mouse Hepa1-6 *Per2-luc* cells were cultured in 15 cm petri dishes until they reached 80% confluency. On the day of tumour inoculation,

the cells were trypsinised and resuspended at a concentration of 10^6 cells/100 μ L in PBS solution alone (Exp 1-2) or with 1:1 MatriGel™ (Corning, Flintshire, UK) (Exp 3-5) and kept on ice until injected.

The mice, aged 8 to 10 weeks, were anesthetized under isoflurane and Hepa 1-6-*Per2-luc* cells were injected subcutaneously in both postero-lateral flanks of each mouse. Mice were then inspected and weighed daily until experiment completion. Tumour sites were inspected daily until tumours became palpable and amenable to daily measurements of perpendicular diameters using callipers. Measurements were always taken at the same circadian time.

Mean daily tumour weight per mouse was calculated as the average volume of the right and left flank tumours according to $(L \times W^2)/2$, where L is the larger and W the smaller perpendicular diameter, and 1 cm^3 corresponds to 1 g. Mice with an estimated tumour weight exceeding 10% of their body weight, or those in poor general condition or losing >15% of their starting body weight were euthanized in compliance with our Home Office Project Licence specifications approved by the Animals in Science Committee (ASC) and Animal Welfare and Ethical Review Body (AWERB).

Experiment objectives and design

All experiments were performed in compliance with the UK relevant laws and institutional guidelines, and were approved by the Animals in Science Committee (ASC) and the Animal Welfare and Ethical Review Body (AWERB) of the University of Warwick.

Exp 1 aimed at the determination of a therapeutic dose of the less soluble FY26.PF₆ formulation. Hepa1-6-bearing nude mice were randomly assigned to be injected intraperitoneally (ip) with vehicle (controls), or 40, 60 or 80 mg/kg/inj of FY26.PF₆ at ZT6 (in the middle of the light span) every other day for 12 days (**Table 1**).

Exp 2 aimed at assessing whether FY26.PF₆ circadian timing would influence toxicity or efficacy in the nude mouse model. The animals were randomly assigned to receive ip vehicle or FY26.PF₆ (50

mg/kg/inj) at ZT6 or at ZT18 (4 controls and 6 treated mice per ZT) every other day for 11 days (6 injections; cumulative dose, 300 mg/kg).

Exp 3 aimed at assessing the efficacy and tolerability of the more soluble formulation of FY26.Cl in Hepa1-6-bearing C57Bl/6 mice. The mice were randomized to receive vehicle or FY26.Cl, at a cumulative dose of 60 mg/kg. Treated mice received ip injections of 20 mg/kg of FY26.Cl at ZT6 12, 14 and 17 days after tumour inoculation. Control mice received ip vehicle on the same days.

Exp 4 aimed at confirming efficacy and optimizing timing and scheduling of the same cumulative dose of 60 mg/kg of FY26.Cl. Mice were randomized to receive either vehicle or FY26.Cl as 4 injections of 15 mg/kg at ZT6 or ZT18 on days 11, 14, 17 and 21.

Exp 5 determined FY26.Cl uptake in mouse tumour and liver. Hepa1-6 bearing mice were randomly assigned to either treatment or control groups. They received a single ip injection of 5, 10, or 20 mg/kg of FY26.Cl or 0.1 M PBS (vehicle) at ZT6 (**Table 1**). The mice from pre-set subgroups were culled at 6, 24 or 48 hours after injection. The subcutaneous tumours in both flanks, as well as liver, spleen, one kidney, an ileum and a colon segment and brain were sampled and stored at -80 °C.

FY26 sample preparation

For Exp 1-2, FY26.PF₆ was diluted in the vehicle, composed of 1% TWEEN 80 (Sigma Aldrich, Gillingham, UK), 5% DMSO (Corning, New York, USA) and 94% of 0.9% saline (Prep room, Life Sciences, University of Warwick) under laminar flow. FY26.PF₆ concentration was confirmed with ICP-MS. For Exp 3-5, using FY26.Cl, a stock solution of 50 mg/mL FY26.Cl was prepared in 0.9% saline on the day of injection and diluted as required; the vehicle consisted of 0.9% saline.

Tissue sample preparation and chemical digestion

Liver tissue was homogenised by manual mechanical grinding (pestle and mortar) whilst frozen under liquid N₂. Once thawed, approximately 90-110 mg of homogenised tissue was pipetted into microwave reaction vessels (10 mL), and tetramethylammonium hydroxide (TMAH, 25% m/v, 2 mL)

was added. Tumour tissue was not homogenised and instead digested as whole tissues. It was weighed directly into microwave vials and TMAH was added (100 μ L per 5 mg tissue, minimum of 500 μ L added). The samples were digested via microwave irradiation (CEM SP-D Discover[®] microwave reactor, ≥ 300 W, ≥ 450 PSI) at 200 °C for 10 min. Digested samples were diluted in 1 part doubly-deionised water (DDIW), then centrifuged at 9000 rpm for 10 min at 20 °C. The final analytical samples were prepared by a further 1 in 12.5 dilution in DDIW (total dilution of 1 in 25), ensuring that the final concentration of TMAH is 1% and the total dissolved solids were $<0.1\%$. TMAH digestion was selected to circumvent the formation of volatile Os species with nitric acid.

ICP-MS analysis

Analyses of digested tissue samples were carried out on an Agilent Technologies ICP-MS 7900 spectrometer in a basic aqueous matrix of TMAH (1%, m/v). The osmium concentrations were determined via isotopic detection of ^{189}Os in gas (He) and no-gas modes, and samples were referenced internally to ^{100}Ru (10 ppb). A concentration calibration curve was produced by serial dilutions of an osmium standard (1000 ppm) in 1% TMAH: 0, 0.1, 0.25, 0.5, 1, 2.5, 5, 10, 25, 50, 100, 250, 500 and 1000 ppb.

Statistical methods

Body weight data were expressed as % body weight measured on the first treatment day. Tumour weights in individually treated mice were expressed as % of the median control values, in order to determine % inhibition. Mean and Std error (SE) or median and interquartiles were computed for the different treatment groups and experimental conditions, i.e., drug timing and day of assessment. Groups were compared using parametric or non-parametric ANOVAs, respectively.

Table 1: Endpoints, and main characteristics of the five mouse experiments (Exp).FY26.PF₆ was used in Exp 1 and 2, while FY26.Cl was administered in Exp 3, 4 and 5.

Exp #	Endpoints	Daily dose (mg/kg) and ZT	N of inj (no. of days between injections)	Cumulative dose given (mg/kg)	Treatment duration (days)	Dose intensity (mg/kg/d)	N of mice Strain (N of treated /controls)
1	Tumour and Body weight changes	40, 60 or 80 (ZT6)	6 (2)	240-480	12	20-40	18 CD1-Foxn1 ^{nu} (15/3)
2	Id.	50 (ZT6 or ZT18)	6 (2)	300	12	25	20 CD1-Foxn1 ^{nu} (12/8)
3	Id.	20 (ZT6)	3 (2-3)	60	5	12	36 C57Bl/6 (20/16)
4	Id.	15 (ZT6 or ZT18)	4 (3-4)	60	10	6	30 C57Bl/6 (20/10)
5	[Os] (ng/g) in tumour, liver, and 5 organs Tumour and body weights	0, 5, 10 or 20 (ZT6)	1 (tissue samples at 6, 24, 48 h)	5 to 20	1	N.A.	66 C57Bl/6 (57/9)
All	-	5 to 80	1 to 6 (2 to 4)	5 to 480	1 to 12	1 to 40	170 (124/46)

ORIGINAL UNEDITED

RESULTS

Comparability of FY26.X maximum solubilities

The maximum aqueous solubilities of FY26.X (where X = PF₆, I, or Cl) were determined in doubly-deionised water. Their solubilities were measured as 0.0201 (± 0.0007), 1.29 (± 0.01), and 215 (± 10) mM for X = PF₆, I and Cl, respectively. A dramatic 10,448-fold increase in solubility is observed by switching the counter-anion from PF₆ to Cl (**Figure 2**).

In vitro antiproliferative activity of FY26.X and its enantiomers

The antiproliferative activity of FY26.X was measured in A2780 ovarian cancer cells, where X, the counter-anion, was varied (PF₆ or Cl, **Figure 3**). The data confirm the lack of any statistically significant difference in anticancer activity between the new highly soluble formulation (X = Cl) and the older formulation (X = PF₆). Furthermore, FY26 has a chiral metal centre and exists as a racemic mixture of two enantiomers as shown by its X-ray crystal structure.²⁴ As previously reported for FY26.PF₆¹⁸, FY26.Cl similarly did not induce apoptosis on exposure in A2780 cells but did induce an increase in reactive oxygen species (data not shown). Herein, the enantiomers were separated via chiral HPLC and individually tested against A2780 ovarian and A549 lung cancer cells (**Figure 3**). The activity of both enantiomers was similar for A549 cells, however, that of one enantiomer was twice as large as that of the other one for A2780 cells.

Dose and time dependencies of FY26.PF6 effects in tumour-bearing nude mice

In **Exp 1** and **2**, tumours grew exponentially up to a median value of *circa* 1.2 and 1 g respectively, which was reached 14 days after inoculation. In **Exp 1**, a dose-response was documented for tumour inhibition, with efficacy ranking as highest for the dose of 80 mg/kg/inj, intermediate for that of 40 mg/kg/inj, and least for 60 mg/kg/inj.²¹ Body-weight loss displayed a linear dose response relation,

with the higher dose being clearly too toxic since all the mice treated at this dose level were euthanized after up to 5 injections (cumulative dose of 400 mg/kg).²¹

In **Exp 2**, tumour growth slowed down transiently after the 6th FY26.PF₆ dose, with a slightly better efficacy at ZT6 (**Figure 4A**). Body-weight loss was less pronounced in the mice treated at ZT6 as compared to ZT18 (**Figure 4B**).

Schedule-dependent anti-tumour efficacy of FY26.Cl in C57Bl/6 mice

The distributions of mean tumour weights per mouse were similar in control and treatment groups both within and between experiments before FY26 treatment in Exp 3 and 4. Indeed, no statistically significant difference was found for comparisons of treatment vs control groups ($p = 0.843$) or for that of Exp 3 vs Exp 4 ($p = 0.671$), and no interaction term was validated, with two-way ANOVA. Large interindividual variations were found however, since the average tumour weight that was measured in each mouse varied by >10-fold in both control and treated groups of each Exp.

The tumour weights in controls nearly doubled over the 8-12 days following the first vehicle administration, but did not exceed 0.25 g, thus indicating a slower tumour growth in the C57B/L6 mice

(Exp 3-4) as compared to the CD1-Foxn1^{nu} (Exp 1-2). Spontaneous partial tumour regressions and regrowth were noticed. Tumours tended to be smaller in the treated mice throughout each Exp, and a clear antitumour effect of FY26.Cl was demonstrated 20 and 23 days after tumour inoculation in Exps 3 and 4, respectively (**Figure 5**). The treated mice in both experiments had then received a cumulative dose of 60 mg/kg over 5 days for Exp 3, and over 10 days for Exp 4. For Exp 3, the median tumour weight was 30.2 mg for the treatment group and 128.8 mg for the control group on day 20 (**Figure 5A**). In Exp 4, these respective values were 122.3 mg (treatment groups ZT6 & ZT18) and 213.2 mg (control group) on day 23 (**Figure 5B**). The higher dose intensity of FY26 was associated with a significantly larger tumour inhibition rate (Kolmogorov-Smirnov test, $p = 0.0217$). Thus, at Exp

completion, the median percentage of FY26.Cl-induced tumour inhibition relative to controls was 76.5% in Exp 3, where the drug was given at ZT6 only, and 42.6% in Exp 4 irrespective of dosing time. At the end of Exp 4, the percentage inhibition relative to control was 12.5% in the mice dosed with FY26.Cl at ZT6 and 66% in those treated at ZT18 (Kruskall Wallis ANOVA, $p=0.022$) (**Figure 5D**). FY26 efficacy, however, could be determined only for those mice that survived the treatment toxicities.

Circadian timing-dependent toxicity of FY26.Cl

Thus, at study completion, 13/20 controls in Exp 3, and 10/10 controls in Exp 4 were alive, representing an overall rate of 23/30 controls for both Exp (76.7%). Seven control mice (23.3%) had to be euthanised due to tumour progression. In contrast, severe clinical toxicity signs were observed that mandated euthanizing nearly half of the treated mice for ethical reasons. As a result, 8/16 (50%) and 9/20 treated mice (45%) were alive at completion of Exp 3 and 4, respectively. In Exp 4, overall survival was best following FY26 dosing at ZT6 as compared to ZT18 with respective survival rates of 60% vs 30% (Gehan-Breslow-Wilcoxon test, $p=0.0012$). Body weight loss, however, did not correlate with other signs of physical condition that triggered humane endpoints.

Daily body weights increased gradually in controls over the respective treatment durations in each experiment. The FY26-treated mice displayed a modest yet consistent decrease in body weight as compared to pre-treatment values in both experiments. Body weight was primarily reduced after the second injection then remained rather stable despite further FY26 administrations (**Figure 6**)

Thus, the body weight changes showed a significant difference between the treated and the control group after the third dose in each Exp. After a cumulative dose of 60 mg/kg of FY26.Cl, mice lost ~10% ($\pm 3.2\%$) of their body weight before treatment. Body weight loss from FY26 dosing was clearly worse at ZT18 as compared to ZT6 (**Figure 6B**). Mann Whitney test validated significant differences in body weight changes between controls and FY26-treated mice over each Exp duration irrespective

of drug timing ($p=0.0017$ and $p=0.0059$, for Exp1 and 2 respectively), as well as for circadian timing effects (Dunnett's multiple comparisons test, $p<0.0001$).

FY26 tumour and liver pharmacokinetics and pharmacodynamic correlations

Following the administration of FY26.Cl to Hepa1-6 *Per2-luc* tumour-bearing mice at ZT6, the tissue [Os] concentrations varied as a function of dose at 6 h, in the tumours in each flank and in liver (**Figure 7**). Based on these data, FY26.Cl tumour uptake was nearly ten-fold less in both tumours as compared to liver at 6 h post treatment.

The tumour [Os] levels remained almost constant over time in the mice dosed with 20 mg/kg, with similar values in the right and left flank tumours sampled at 6, 24 and 48 h after injection (**Figure 7A-B**). In contrast the [Os] in the tumours of both flanks decreased at 24 h and slightly increased at 48 h for both lower dose levels (10 and 5 mg/kg). In the liver, similar [Os] concentrations were found 6 h after dosing the mice with 20 or 10 mg/kg, while [Os] levels nearly halved in the mice treated with 5 mg/kg (**Figure 7C**). Liver [Os] levels remained almost constant until 48 h for the mice treated with 20 mg/kg of FY 26.Cl. In contrast, the liver [Os] concentrations decreased sharply at 24 h and remained stable until 48 h for the 10 and 5 mg/kg doses.

Taken together, these tissue pharmacokinetics data suggest that some uptake saturation mechanisms and efflux blockage for at least 48 h are reached both in the tumour and in the liver with a single ip dose of 20 mg/kg of FY26.Cl. The partial clearance of liver Os at 24 h in the mice dosed with 10 or 5 mg/kg could result in Os re-uptake by the tumours from the bloodstream, hence accounting for the slight tumour [Os] increase at 48 h, and might possess a better therapeutic index.

All the treated mice lost some weight 24 and or 48 h post dosing, while controls gained some weight over this time span. Nevertheless, body weight changes were $<5\%$ in all the mice, whatever the dose

level and day of assessment. The limited sample size and low toxicity of a single dose precluded the demonstration of any dose-response relationship, using body weight changes as an endpoint. No changes in tumour volumes were found, as expected following a single FY26 dose.

DISCUSSION

Currently, the most widely administered drugs in cancer chemotherapy are platinum complexes (cisplatin, carboplatin and oxaliplatin).²⁵ Despite the clinical efficacy of these drugs, there is a need for new drugs with different mechanisms of action which can circumvent platinum resistance, widen the spectrum of activity, and reduce side effects.²⁶

Organo-osmium anticancer complexes with PF₆ anions have high crystal packing energies, and we previously reported that solubility can be improved up to 45-fold by switching to CF₃SO₃ anions.²² Here we show that FY26.X solubility is vastly improved 10,448-fold by switching to a chloride anion. Such drastic solubility improvements eliminate the need for DMSO in biological assays and improve viability for clinical use. Furthermore, since the active component is the organo-osmium cation, the change in anion did not significantly alter its pharmacological activity.

Amongst other precious metals, complexes of Os(II), also a 3rd row transition metal, and isoelectronic with Pt(IV), show promise. Here we have studied the organo-osmium(II) half-sandwich complex FY26 ([Os^{II}(η^6 -*p*-cym)(PhAzPy-NMe₂))I]⁺ a pseudo-octahedral complex in which the arene, *p*-cymene occupies 3 coordination positions, the phenylazopyridine ligand is chelated, and a strongly bound iodide ligand completes the coordination sphere.²⁷

FY26 is a relatively inert complex that does not readily hydrolyse even after 24 h incubation at 37° C in aqueous solution at pH 7.4, or react with DNA bases.¹² However, radiolabelling studies with ¹³¹I have shown that the complex is activated in cancer cells and the iodide ligand is rapidly excreted.¹⁶ The activation of FY26 appears to involve attack of the azo-bond of the chelated ligand by the

abundant intracellular tripeptide glutathione, which weakens the Os-I bond.¹⁷ This complex appears to act as a metabolic inhibitor, inducing cell apoptotic death via ROS generation.^{3, 4} The mechanism also involves the arrest of cycling cells in G1-phase, thus halting cellular proliferation.¹²

Here, a consistent yet moderate efficacy of the osmium complex FY26 was demonstrated in hepatocarcinoma-bearing mice, as indicated with a circa 60% tumour inhibition as compared to controls using the more soluble FY26.Cl. Indeed, both FY26.Cl and the FY26.PF₆ displayed some efficacy in this tumour model, both *in vitro* and *in vivo*.²¹ Reaching a cumulative dose of 60 mg/kg appeared to be necessary for FY26.Cl efficacy to become apparent.

Since the circadian clock regulates both cellular metabolism and the cell cycle,^{6,7} we sought whether circadian timing would moderate FY26 effects in this mouse hepatocarcinoma model, both in cell cultures and in tumour-bearing mice, and aimed at the determination of implications for optimization of treatment schedules.

The dosing time of FY26 significantly impacted on FY26 tolerability, as indicated by the loss in body weight of the tumour bearing mice. The mice treated at ZT18 showed larger loss in body weight as compared to those treated at ZT6. This was consistent both in the current studies using FY26.PF₆ or FY26.Cl, and in prior experiments where FY26.PF₆ had been administered at six ZT's in non tumour-bearing mice.²¹

The blockbuster platinum complex oxaliplatin has largely benefitted from circadian research early on, at a time when its development as an anticancer drug had been halted for undue clinical toxicities.²⁸ More specifically, the toxicities of oxaliplatin, like those of carboplatin and cisplatin, were halved or reduced even more through their administration in mice or rats during their nocturnal activity span.^{29, 30} Interestingly, the antitumour efficacy of both cisplatin and oxaliplatin

were enhanced following dosing at the time when both drugs were least toxic.^{31, 32} Moreover, early afternoon delivery of oxaliplatin significantly improved tolerability and efficacy of oxaliplatin in metastatic colorectal cancer patients.^{9, 33} Reduced glutathione plays a key role in the circadian detoxification mechanisms of the platinum complexes. Thus the cytosolic concentrations of reduced glutathione more than doubled along the 24-hour time scale in mouse liver with a statistically significant circadian rhythm.³⁴ The 24-hour mean of GSH concentrations was more than halved following the administration of L-buthionine sulfoximine (L-BSO), an inhibitor of gamma-glutamylcysteine synthetase, a rate limiting enzyme of GSH synthesis. Moreover the GSH pattern became bimodal over the 24 hours after L-BSO exposure. The rhythmic patterns in cisplatin toxicities closely matched those in GSH. Thus the prominent circadian rhythm that characterized cisplatin^{29, 30} was drastically altered in the BSO-treated mice, with a 5.7 fold reduction in average survival rate, and a shift in the period of cisplatin toxicity rhythm from 24-h to 12-h.³⁵ Reduced glutathione, however, appeared to have a dual role for FY26 pharmacology, i.e. it can facilitate the bioactivation of FY26 into the corresponding aqua-species, but also detoxify cells from the chloride adduct FY26. This may account for the several hours' difference regarding the circadian times of administration that optimize the tolerability of platinum complexes on the one hand, and of FY26 on the other hand, both *in vitro* and *in vivo*.^{21, 29, 30}

In spite of the larger body weight loss, the mice receiving FY26.Cl at ZT18 had a larger tumour weight reduction as compared to those injected at ZT6. The apparent increase in antitumour efficacy following dosing at the circadian time of poor tolerability strikingly differs from prior findings with other anticancer agents including cisplatin and oxaliplatin. Thus, the dosing time of best efficacy coincided with that of best tolerability for 28 anticancer drugs.⁶⁻⁸ However, spontaneous regressions and regrowth characterized the experimental model we used here, thus indicating the occurrence of host immunologic responses against the subcutaneous Hepa 1-6 tumours, which were growing in genetically-related yet non syngeneic mice (C57Bl/6 instead of C57L/J).^{34, 36} Our study suggests that

treatment schedules should indeed aim to reduce the exposure of healthy tissues to FY26.Cl through drug dosing at ZT6, because (i) a significant tumour drug uptake was demonstrated at this time, (ii) a significant tumour inhibition was achieved in mice treated at this time with the more dose intensive schedule (Exp 3), and (iii) the optimization of drug tolerability was crucial for outcomes (Exp 4).

Conclusions

Here, we have demonstrated that FY26.Cl and FY26.PF₆ are least toxic to the mice, following dosing near the middle of their resting span, during daytime. The circadian pattern in the FY26.Cl tolerability that was found here, was similar to that demonstrated earlier for the less soluble FY26.PF₆ formulation. The circadian optimization of tolerability appeared potentially useful, because FY26-induced antitumour efficacy required treatment with repeated administrations. Thus good tolerability would favor compliance to the subchronic treatment that was needed to achieve efficacy. Since the tumour drug levels remained similar at 48 h-post dose, irrespective of dose level, we propose to enhance treatment efficacy through the daily delivery of low dose levels (i.e., 5-10 mg/kg) at ZT6, a high dose intensity schedule which could be automatically delivered using “intelligent” nanoparticles.

CONFLICTS OF INTEREST

SK, KA, HM, LG, RN, HB, RD, SB, PS and FL declared no conflict of interest.

ACKNOWLEDGEMENTS

We thank the CRUK (grant no. NS/A000031/1, C53561/A19933), EPSRC (grant nos. EP/F034210/1 and EP/P030572/1), and Anglo American Platinum for support, and Dr Lijiang Song for assistance with ICP-MS.

Figure 1. Schemes of FY26 molecular structures and action mechanisms. (A) Structure of the organo-osmium azopyridine complex FY26 and abbreviations used for the PF_6^- and Cl^- salts. (B) Proposed biomolecular mechanisms for the cytotoxicity of FY26 involving intracellular activation by GSH-induced hydrolysis, calcium mobilization, mitochondrial dysfunction, ROS generation, and cell death.³⁷

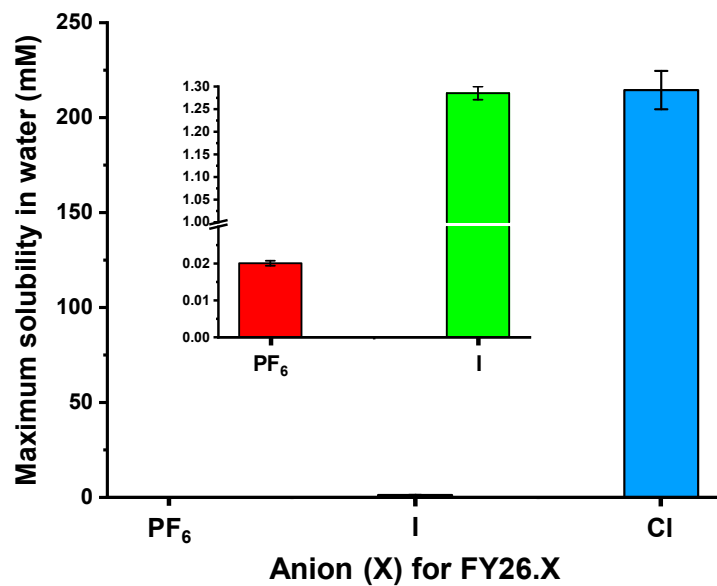


Figure 2. Bar graph of the dependence of the maximum solubilities of FY26.X on the anion X, in water (where X = PF₆⁻, I⁻ or Cl⁻). Data are mean ±SD of N=3, being 0.0201 (± 0.0007), 1.29 (± 0.1), and 215 (± 10) mM for FY26.PF₆, FY26.I, and FY26.Cl, respectively.

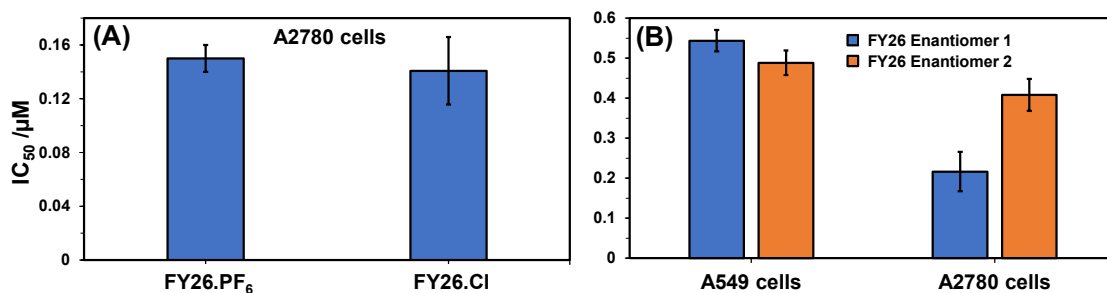


Figure 3. Bar-graphs illustrating the *in vitro* anticancer efficacy of different forms of FY26. (A) Antiproliferative activities of FY26.PF₆ and FY26.Cl against A2780 cancer cells. Data represent Mean \pm SD of N=6. (B) Antiproliferative activities of the FY26 enantiomers against A2780 and A549 cancer cells. Mean \pm SD of N=6.

Figure 4: Dosing time effects of FY26 in Hepa1-6-bearing nude mice (Exp 2). Effects of FY26.PF6 (50 mg/kg/inj) on tumour weights (A), and body weight changes (B), according to injection timing (Zeitgeber Time). Data shown in panels A and B are median \pm Interquartile range (IQR's).

Figure 5: Antitumour efficacy of FY26.Cl in Hepa1-6-bearing C57Bl/6 mice. Growth curves of inoculated Hepa1-6 Per2-luc tumours in male C57Bl/6 mice treated with vehicle (control groups) or FY26.Cl (treated groups). Median daily tumour volumes (\pm interquartiles) in treated mice or controls receiving vehicle. (A) Exp 3, with mice in treated group with 20 mg/kg of FY26.Cl i.p per injection x 3 injections. (B) Exp 4, with mice in treated group dosed with 15 mg/kg of FY26.Cl ip per injection x 4 injections. (C) FY26.Cl induced tumour weight (%) inhibition relative to median control tumour weight. (D) Tumour weight inhibition (%) relative to median control tumour weight, according to FY26.Cl timing. Data shown in panels C and D are median \pm Interquartile range (IQR)

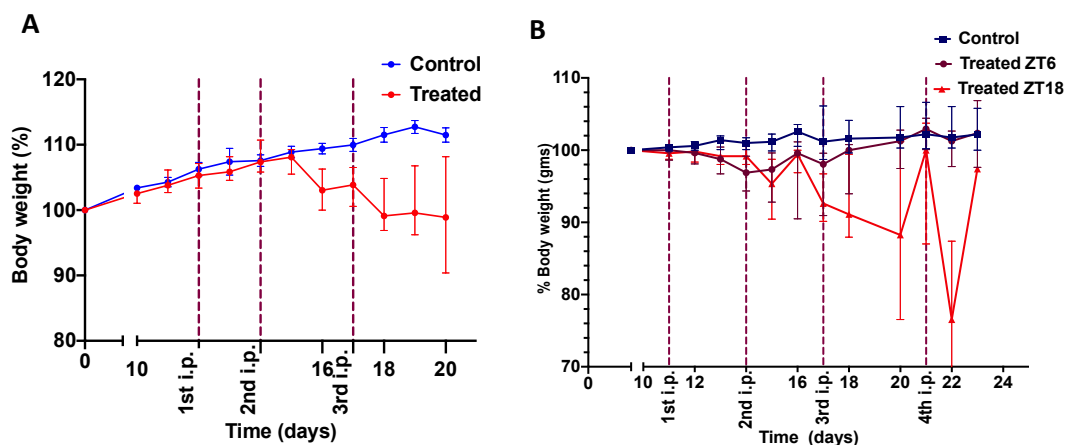


Figure 6: Relative changes in body weight following vehicle (control groups) or FY26.Cl (treated groups) administration in Hepa1-6 Per2-luc tumour-bearing mice treated in two experiments.

Median daily body weight (\pm interquartiles). (A) Exp 3, mice in treated group receiving 20 mg/kg of FY26 i.p per injection \times 3 injections at ZT6. (B) Exp 4, mice in treated group dosed with 15 mg/kg of FY26 ip per injection \times 4 injections at ZT6 or ZT18.

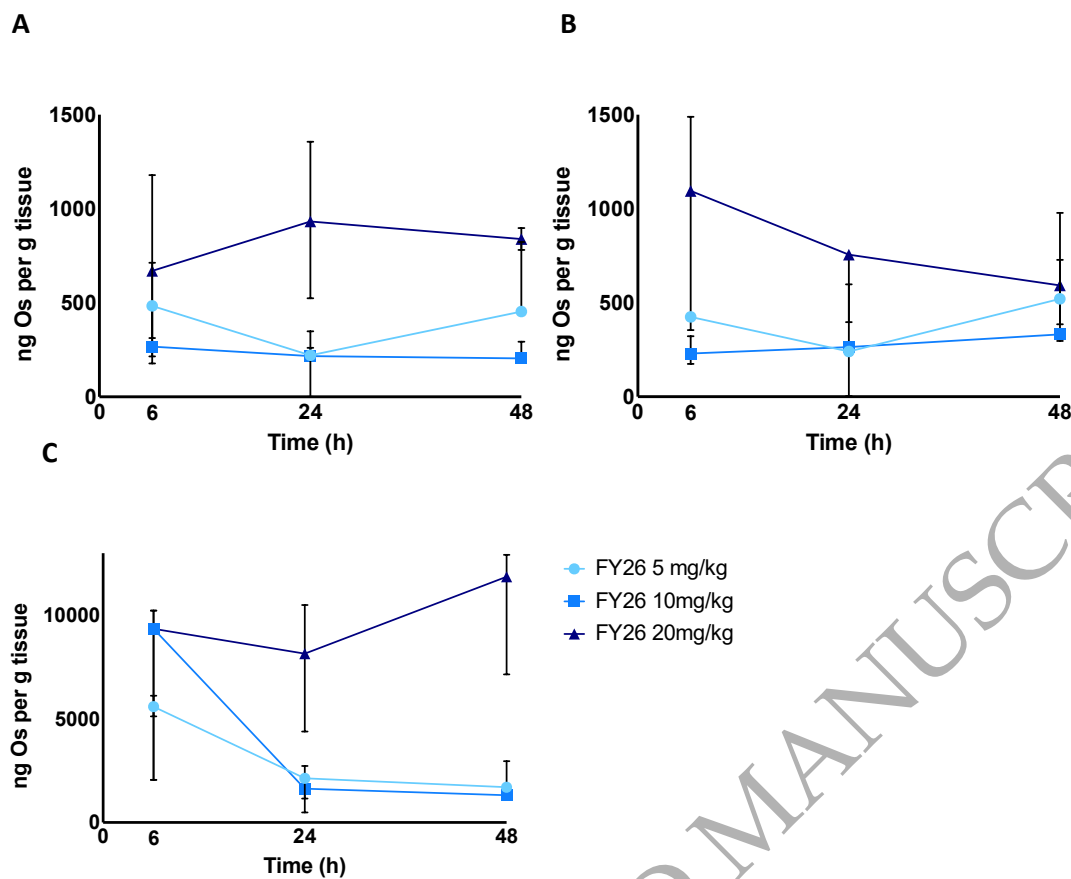


Figure 7: Dose-dependent kinetics of osmium concentrations in tumour and liver tissues from mice (N=3). A) left tumour; B) right tumour; C) liver. All data points are median \pm interquartile range (IQR).

REFERENCES

1. Hartinger, C. G.; Zorbas-Seifried, S.; Jakupec, M. A.; Kynast, B.; Zorbas, H.; Keppler, B. K., From bench to bedside – preclinical and early clinical development of the anticancer agent indazolium trans-[tetrachlorobis(1H-indazole)ruthenate(III)] (KP1019 or FFC14A). *J. Inorg. Biochem.* **2006**, *100* (5), 891-904.
2. Leijen, S.; Burgers, S. A.; Baas, P.; Pluim, D.; Tibben, M.; van Werkhoven, E.; Alessio, E.; Sava, G.; Beijnen, J. H.; Schellens, J. H. M., Phase I/II study with ruthenium compound NAMI-A and gemcitabine in patients with non-small cell lung cancer after first line therapy. *Invest. New Drugs* **2015**, *33* (1), 201-214.
3. Meier-Menches, S. M.; Gerner, C.; Berger, W.; Hartinger, C. G.; Keppler, B. K., Structure-activity relationships for ruthenium and osmium anticancer agents - towards clinical development. *Chem Soc Rev* **2018**, *47* (3), 909-928.
4. Johnstone, T. C.; Suntharalingam, K.; Lippard, S. J., Third row transition metals for the treatment of cancer. *Philos Trans A Math Phys Eng Sci* **2015**, *373* (2037).
5. Pizarro, A. M.; Habtemariam, A.; Sadler, P. J., Activation Mechanisms for Organometallic Anticancer Complexes. In *Medicinal Organometallic Chemistry*, Jaouen, G.; Metzler-Nolte, N., Eds. Springer Berlin Heidelberg: Berlin, Heidelberg, 2010; pp 21-56.
6. Dallmann, R.; Okyar, A.; Levi, F., Dosing-Time Makes the Poison: Circadian Regulation and Pharmacotherapy. *Trends Mol Med* **2016**, *22* (5), 430-45.
7. Okyar, A.; Kumar, S. A.; Filipinski, E.; Piccolo, E.; Ozturk, N.; Xandri-Monje, H.; Pala, Z.; Abraham, K.; Gomes, A. R. G. d. J.; Orman, M. N.; Li, X.-M.; Dallmann, R.; Lévi, F.; Ballesta, A., Sex-, feeding-, and circadian time-dependency of P-glycoprotein expression and activity - implications for mechanistic pharmacokinetics modeling. *Scientific Reports* **2019**, *9* (1), 10505.
8. Levi, F.; Okyar, A.; Dulong, S.; Innominato, P. F.; Clairambault, J., Circadian timing in cancer treatments. *Annu Rev Pharmacol Toxicol* **2010**, *50*, 377-421.
9. Levi, F.; Focan, C.; Karaboue, A.; de la Valette, V.; Focan-Henrard, D.; Baron, B.; Kreutz, F.; Giacchetti, S., Implications of circadian clocks for the rhythmic delivery of cancer therapeutics. *Adv Drug Deliv Rev* **2007**, *59* (9-10), 1015-35.
10. Innominato, P. F.; Ballesta, A.; Huang, Q.; Focan, C.; Chollet, P.; Karaboue, A.; Giacchetti, S.; Bouchahda, M.; Adam, R.; Garufi, C.; Levi, F. A., Sex-dependent least toxic timing of irinotecan combined with chronomodulated chemotherapy for metastatic colorectal cancer: Randomized multicenter EORTC 05011 trial. *Cancer Med* **2020**, *9* (12), 4148-4159.
11. Fu, Y.; Habtemariam, A.; Basri, A. M. B. H.; Braddick, D.; Clarkson, G. J.; Sadler, P. J., Structure-activity relationships for organometallic osmium arene phenylazopyridine complexes with potent anticancer activity. *Dalton Trans.* **2011**, *40*, 10553-10562.
12. Fu, Y.; Habtemariam, A.; Pizarro, A. M.; van Rijt, S. H.; Healey, D. J.; Cooper, P. A.; Shnyder, S. D.; Clarkson, G. J.; Sadler, P. J., Organometallic Osmium Arene Complexes with Potent Cancer Cell Cytotoxicity. *J. Med. Chem.* **2010**, *53* (22), 8192-8196.
13. Shnyder, S. D.; Fu, Y.; Habtemariam, A.; van Rijt, S. H.; Cooper, P. A.; Loadman, P. M.; Sadler, P. J., Anti-colorectal cancer activity of an organometallic osmium arene azopyridine complex. *MedChemComm* **2011**, *2* (7), 666-668.

14. Kostrhunova, H.; Florian, J.; Novakova, O.; Peacock, A. F.; Sadler, P. J.; Brabec, V., DNA interactions of monofunctional organometallic osmium(II) antitumor complexes in cell-free media. *J Med Chem* **2008**, *51* (12), 3635-43.
15. Zhang, P.; Huang, H., Future potential of osmium complexes as anticancer drug candidates, photosensitizers and organelle-targeted probes. *Dalton Trans* **2018**, *47* (42), 14841-14854.
16. Needham, R. J.; Sanchez-Cano, C.; Zhang, X.; Romero-Canelon, I.; Habtemariam, A.; Cooper, M. S.; Meszaros, L.; Clarkson, G. J.; Blower, P. J.; Sadler, P. J., In-Cell Activation of Organo-Osmium(II) Anticancer Complexes. *Angew Chem Int Ed Engl* **2017**, *56* (4), 1017-1020.
17. Zhang, X.; Ponte, F.; Borfecchia, E.; Martini, A.; Sanchez-Cano, C.; Sicilia, E.; Sadler, P. J., Glutathione activation of an organometallic half-sandwich anticancer drug candidate by ligand attack. *Chem. Commun.* **2019**, *55* (97), 14602-14605.
18. Hearn, J. M.; Romero-Canelón, I.; Munro, A. F.; Fu, Y.; Pizarro, A. M.; Garnett, M. J.; McDermott, U.; Carragher, N. O.; Sadler, P. J., Potent organo-osmium compound shifts metabolism in epithelial ovarian cancer cells. *Proceedings of the National Academy of Sciences* **2015**, *112* (29), E3800-E3805.
19. Romero-Canelón, I.; Mos, M.; Sadler, P. J., Enhancement of Selectivity of an Organometallic Anticancer Agent by Redox Modulation. *J. Med. Chem.* **2015**, *58* (19), 7874-7880.
20. Abraham K., Dallmann R., Ballesta A., Romero-Canelon I. Sadler P.J., Lévi F.A.: *In vitro circadian synchronisation of mouse hepatocarcinoma cells with 24h temperature cycles uncovers in vitro chronotoxicity of novel anticancer drug.*, Proc 15th Congress of the European Biological Rhythms Society, Amsterdam (NL), Amsterdam (NL), 2018: Abstr. P68.
21. Abraham, K. In vitro and in vivo chronopharmacology of a new generation of an organometallic anticancer drug complex. University of Warwick, Coventry, United Kingdom, 2018.
22. Needham, R. J.; Bridgewater, H. E.; Romero-Canelón, I.; Habtemariam, A.; Clarkson, G. J.; Sadler, P. J., Structure-activity relationships for osmium(II) arene phenylazopyridine anticancer complexes functionalised with alkoxy and glycolic substituents. *J. Inorg. Biochem.* **2020**, 111154.
23. Vichai, V.; Kirtikara, K., Sulforhodamine B colorimetric assay for cytotoxicity screening. *Nat Protoc* **2006**, *1* (3), 1112-6.
24. Needham, R. J.; Sanchez-Cano, C.; Zhang, X.; Romero-Canelón, I.; Habtemariam, A.; Cooper, M. S.; Meszaros, L.; Clarkson, G. J.; Blower, P. J.; Sadler, P. J., In-Cell Activation of Organo-Osmium(II) Anticancer Complexes. *Angew. Chem. Int. Ed.* **2017**, *56* (4), 1017-1020.
25. Arnesano, F.; Losacco, M.; Natile, G., CHAPTER 15 Platinum. In *Binding, Transport and Storage of Metal Ions in Biological Cells*, The Royal Society of Chemistry: 2014; pp 429-460.
26. Hanif, M.; Babak, M. V.; Hartinger, C. G., Development of anticancer agents: wizardry with osmium. *Drug Discov Today* **2014**, *19* (10), 1640-8.
27. Noffke, A. L.; Habtemariam, A.; Pizarro, A. M.; Sadler, P. J., Designing organometallic compounds for catalysis and therapy. *Chemical Communications* **2012**, *48* (43), 5219-5246.
28. Cederroth, C. R.; Albrecht, U.; Bass, J.; Brown, S. A.; Dyhrfeld-Johnsen, J.; Gachon, F.; Green, C. B.; Hastings, M. H.; Helfrich-Forster, C.; Hogenesch, J. B.; Levi, F.; Loudon, A.;

- Lundkvist, G. B.; Meijer, J. H.; Rosbash, M.; Takahashi, J. S.; Young, M.; Canlon, B., Medicine in the Fourth Dimension. *Cell Metab* **2019**, *30* (2), 238-250.
29. Boughattas, N. A.; Levi, F.; Fournier, C.; Hecquet, B.; Lemaigre, G.; Roulon, A.; Mathe, G.; Reinberg, A., Stable circadian mechanisms of toxicity of two platinum analogs (cisplatin and carboplatin) despite repeated dosages in mice. *J Pharmacol Exp Ther* **1990**, *255* (2), 672-9.
30. Boughattas, N. A.; Levi, F.; Fournier, C.; Lemaigre, G.; Roulon, A.; Hecquet, B.; Mathe, G.; Reinberg, A., Circadian rhythm in toxicities and tissue uptake of 1,2-diamminocyclohexane(trans-1)oxalatoplatinum(II) in mice. *Cancer Res* **1989**, *49* (12), 3362-8.
31. Sothorn, R. B.; Levi, F.; Haus, E.; Halberg, F.; Hrushesky, W. J., Control of a murine plasmacytoma with doxorubicin-cisplatin: dependence on circadian stage of treatment. *J Natl Cancer Inst* **1989**, *81* (2), 135-45.
32. Granda, T. G.; D'Attino, R. M.; Filipinski, E.; Vrignaud, P.; Garufi, C.; Terzoli, E.; Bissery, M. C.; Levi, F., Circadian optimisation of irinotecan and oxaliplatin efficacy in mice with Glasgow osteosarcoma. *Br J Cancer* **2002**, *86* (6), 999-1005.
33. Levi, F.; Zidani, R.; Misset, J. L., Randomised multicentre trial of chronotherapy with oxaliplatin, fluorouracil, and folinic acid in metastatic colorectal cancer. International Organization for Cancer Chronotherapy. *Lancet* **1997**, *350* (9079), 681-6.
34. Grimm, C. F.; Ortmann, D.; Mohr, L.; Michalak, S.; Krohne, T. U.; Meckel, S.; Eisele, S.; Encke, J.; Blum, H. E.; Geissler, M., Mouse alpha-fetoprotein-specific DNA-based immunotherapy of hepatocellular carcinoma leads to tumor regression in mice. *Gastroenterology* **2000**, *119* (4), 1104-12.
35. Li, X. M.; Metzger, G.; Filipinski, E.; Boughattas, N.; Lemaigre, G.; Hecquet, B.; Filipinski, J.; Levi, F., Pharmacologic modulation of reduced glutathione circadian rhythms with buthionine sulfoximine: relationship with cisplatin toxicity in mice. *Toxicol Appl Pharmacol* **1997**, *143* (2), 281-90.
36. Kroger, A.; Ortmann, D.; Krohne, T. U.; Mohr, L.; Blum, H. E.; Hauser, H.; Geissler, M., Growth suppression of the hepatocellular carcinoma cell line Hepa1-6 by an activatable interferon regulatory factor-1 in mice. *Cancer Res* **2001**, *61* (6), 2609-17.
37. Sanchez-Cano, C.; Romero-Canelon, I.; Yang, Y.; Hands-Portman, I. J.; Bohic, S.; Cloetens, P.; Sadler, P. J., Synchrotron X-Ray Fluorescence Nanoprobe Reveals Target Sites for Organo-Osmium Complex in Human Ovarian Cancer Cells. *Chemistry* **2017**, *23* (11), 2512-2516.